Construction and Building Materials 153 (2017) 740–750

Contents lists available at ScienceDirect

Construction and Building Materials

journal homepage: www.elsevier.com/locate/conbuildmat

Effect of PCE-type superplasticizer on early-age behaviour of ultra-high performance concrete (UHPC)

P.P. Li [a,b], Q.L. Yu [b,*], H.J.H. Brouwers [a,b]

[a] State Key Laboratory of Silicate Materials for Architectures, Wuhan University of Technology, Wuhan 430070, PR China
[b] Department of the Built Environment, Eindhoven University of Technology, P.O. Box 513, 5600 MB Eindhoven, The Netherlands

HIGHLIGHTS

- Early-age behaviours of UHPC incorporated different dosages of four PCE-type SPs are measured.
- Dispersing and fluid-retaining mechanisms of SP on UHPC are identified by zeta potential, flow and water demand.
- The retardation effect is analysed by setting time, hydration kinetics and early-age strength.
- Different influence of SP on setting time, hydration and shrinkage are explained by physical and chemical process.
- The effects of clay, w/p, nano-silica on SP's dispersing ability are discussed.

ARTICLE INFO

Article history:
Received 6 April 2017
Received in revised form 10 July 2017
Accepted 17 July 2017

Keywords:
Ultra-high performance concrete
PCE superplasticizers
Early-age behaviour
Dispersing ability
Fluid-retaining ability
Retardation effect
Shrinkage

ABSTRACT

The effect of PCE-type SP on zeta potential of particles, spread flow, hydration kinetics, setting time, autogenous shrinkage and chemical shrinkage of UHPC pastes is investigated, as well as the spread flow, slump life and early-age strength development of UHPC. Furthermore, the dispersing and fluid-retaining ability of SP, retardation effect of SP, physical and chemical process effects are analysed. The results show that the dispersing ability of PCE-type SP is determined by its chemical structure, which shows an exponential relationship between the flowability of pastes and SP dosages. The fluid-retaining abilities of UHPCs are sensitive to the water-to-powder ratio, while the further addition of SP will not enhance the slump life after excessing the saturation dosage. Both the adsorbed PCE and the PCE remaining in the aqueous phase contribute to retardation effect. A linear correlation between the final setting time (t_{final}) and the time of maximum heat flow rate ($t_{\dot{Q}=max}$) is derived. The types and dosages of SP primarily influence the absolute chemical shrinkage of pastes within 1 day, but have a great effect on the autogenous shrinkage due to different physical coagulation and chemical process.

1. Introduction

Compared to conventional concrete, ultra-high performance concrete (UHPC) has superior mechanical strength, durability and impact resistance [1–7]. These excellent material properties can be achieved by certain methods, such as eliminating coarse aggregate and using high content of powders to increase the homogeneity [1], optimizing the grain-size distribution of raw materials to improve the compactness [8], utilizing special heat curing or compressing treatments [9], adding high strength fibres [10], etc. Besides those principles, limiting the porosity by using low water-to-powder ratio (w/p) in concretes is probably the most convenient and efficient way to realize those superior material properties. Nevertheless, too low water addition causes the fluidity problem for fresh concrete.

Plasticizers are used to increase the fluidity of concrete with a relatively low addition of water. Since introduction of application in the 1930s, they have been used as critical chemical admixtures for modern concrete [11]. The molecules are adsorbed onto particles, which are then physically separated by opposing their attractive forces with steric and/or electrostatic forces [12,13]. As the first generation water reducer, Lignosulfonates (LS) can limit water content by about 10% [11]. The polymelamine sulfonate (PMS) and sulfonated melamine formaldehyde condensate (SMF) have been produced as the second generation dispersant since 1960s, with a water-reduction ability of about 20–30% [14]. The polycarboxylic ethers (PCEs) based superplasticizers, developed as the new generation in 1980 s, can achieve up to 40% water reduction [15]. Until now, more and more researchers focus on the mechanism of

* Corresponding author.
E-mail address: q.yu@bwk.tue.nl (Q.L. Yu).

http://dx.doi.org/10.1016/j.conbuildmat.2017.07.145
0950-0618/

PCE-type SPs because of their excellent water reduction ability compared to other types of SP [15]. Some mechanisms and effect of PCE-type SP on fresh behaviours of cementitious materials have been revealed, such as chemical structure, adsorption, rheological behaviour and retardation effect [11,16]. However, systematic studies on the effect of PCEs on early-age behaviour of UHPC are still very limited and needed because of the complex influential parameters of those PCE polymers, such as chemistry and length of the backbone, number and length of the side chains, amount of anionic and ionic groups, bond type between backbone and side chain, and overall charge density [11,17–19]. Meanwhile, most researches just focus on cement paste or self-compacting concrete under relatively high water-to-powder ratios. But large amount of powders and very low water content are usually used in UHPC. Therefore, it is necessary to study the effect of PCEs on early-age behaviours of UHPC under very low w/p. To better understand the influence of PCEs, the early-age behaviours should be researched from particle to paste, and then to concrete.

Generally, the early-age behaviours of UHPC can be interpreted by the following parameters: charge characteristics, workability, hydration kinetics, setting time, chemical and autogenous shrinkage, strength development [20]. The workability of UHPC can be described by the initial spread flow and fluid-retaining ability (slump flow life), mainly determined by dispersing ability and retention of superplasticizers [15,21,22], and mineral admixtures [23–28]. The retardation effect is generally defined as the delay of hydration, which can be changed with different adsorption amounts on particles, concentrations of carboxylic in the aqueous phase, and charge characteristics of SP [15,17,29]. Setting time is usually described as a percolation process in forming hydration products to connect the isolated or weakly bound particles [30,31]. This stiffening process is greatly influenced by cement size and w/p, as well as stability of bond between backbone and side chain of SP at alkaline environment [21,32,33]. The chemical shrinkage occurs during the cement hydration because of the smaller volume of the hydration products than that of the raw materials. When concrete is sealed, the autogenous shrinkage is resulting from internal consumption of moisture due to hydration [34,35]. The chemical and autogenous shrinkages are particularly high at early ages of UHPC, due to the usage of low w/p and high content of fine cementitious materials. However, the early-age properties are often discussed alone, the investigation on the correlation between the early-age properties is very limited. Therefore, it is necessary to analyse the correlation between different features.

The objective of this study is to investigate and understand the effect and mechanism of PCE superplasticizer's type and dosage on the early-age behaviours of UHPC. The dispersing ability, fluid-retaining ability and retardation effect of PCEs, as well as physical coagulation and chemical process with PCEs are discussed by using zeta potential, spread flow, water demand, slump life, hydration kinetics, setting time, shrinkages, and early-age strength development. Furthermore, influential factors on superplasticizer's action effects and dispersing effectiveness are illustrated and analysed, such as fine aggregate with clay, water-to-powder ratio, content of nano-material, etc.

2. Experimental program

2.1. Materials

The raw materials used in this study were Portland Cement CEM I 52.5R (PC), limestone powder (LP), nano-silica (nS), micro-sand 0–1 (MS), sand 0–2 (S), water (W) and superplasticizers (SP). The particle size distributions of the used materials were measured by the sieve and laser diffraction analyses using Malvern Mastersizer 2000®, shown in Fig. 1. The chemical compositions of used powders were tested by X-ray Fluorescence (XRF), shown in Table 1.

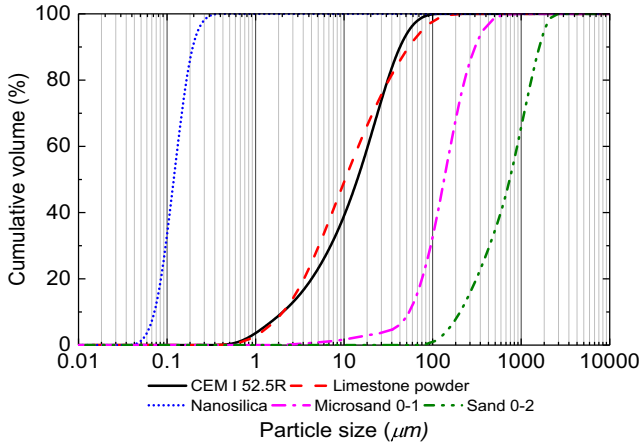

Fig. 1. Particle size distribution of raw materials.

Four PCE-type superplasticizers with different dispersing and retarding abilities were used in the pastes and UHPC, which were provided by different producers. SP1 is synthesized with long side chains. SP2 has a rapid absorption to the cement particles and covers less surface, which ensures a large surface of cement particles to react with water and then accelerates the cement hydration. SP3 can be used to get a very high fluidity and long retention of rheology, even at low water-to-cement ratio. SP4 is suitable for UHPC, which adsorbs on the cement particle with long flexible side chains. The product information (taken from datasheet of supplier) of the superplasticizers are shown in Table 2. The molecular weight of the SPs were measured by gel permeation chromatography (GPC) and the results (molecular weight (Mw) and polydispersity index (PDI)) are provided in Table 2.

Fourier transform infrared spectroscopy (FTIR) tests were performed (Varian 3100F-IR spectrometer) with the wavenumbers ranging from 4000 to 400 cm^{-1} at a resolution of 1 cm^{-1} to characterize the chemical structures, shown in Fig. 2. The FTIR spectrum of the four PCEs are very similar in both wavenumber and intensity, which indicates that the primary functional groups of the PCEs are the same. The O—H stretching vibration is evidently shown at around 3200–3400 cm^{-1}. The other common absorption peaks appear at around 2920 cm^{-1} (C—H stretching), 2880 cm^{-1} (C—H stretching), 1640 cm^{-1} (C=O stretching), 1460 cm^{-1} (C — H bending), 1350 cm^{-1} (C —H bending), 1250 cm^{-1} (C—O stretching), 1080 cm^{-1} (C —O—C stretching) and 950 cm^{-1} (=C—H bending), respectively. While, the SP1 also shows some different infrared absorption peaks at around 1550 cm^{-1} (C=C stretching) and 1410 cm^{-1} (C—H bending).

2.2. Mixture proportions

The mass proportion of paste and UHPC reference admixture in this study is provided in Table 3, following previous research [8]. The nano-silica to binder mass ratio and limestone-to-powder mass ratio was fixed at 4% and 30% respectively in all mixtures. The micro-sand to powder ratio and sand-to-powder ratio was fixed at 0.25 and 1.2, respectively, for all UHPC mixtures. The research parameters of the reference mixture include the SP type and dosage and w/p. The totally used water includes the water in the nano-silica slurry and SP, and the added tap water. The w/p is fixed at 0.2 for the study of spread flow, slump life, hydration kinetic, setting time, shrinkage and strength. While, to evaluate water content sensitivity on slump life, the w/p ratio of 0.22 at SP dosage of 2.2% also investigated. The dosages of SP were determined by the dry matter weight, based on the total mass of all powders.

The mixing of pastes lasted about 5 min using a 5-liter Hobart mixer, following the procedure: dry mixing of the solids for 30 s at the low speed, sequentially adding nano-silica slurry, 80% water, and remaining water incorporated with SP for about total 2 min at the low speed, followed by mixing the paste for 2 min at the low speed and 30 s at the medium speed. The adding order of components in mixing procedure of UHPC was similar to that of paste, whereas the total time is about 8 min (30 s for dry mixing, 180 s for adding slurries and water, another 150 s at the low speed and 120 s at the medium speed).

2.3. Testing methods

2.3.1. Zeta potential

To study the charge characteristics of the suspended particles and determine the adsorption of the PCE-type SPs, zeta potential measurements were conducted by using a Malvern Zetasizer at the set temperature of 25 °C. Diluted slurries were prepared by dissolving 0.1 g of powder (PC, LP, nS) in 100 mL deionized water with

Table 1
Chemical composition of powders.

Substance (%)	CaO	SiO_2	Al_2O_3	Fe_2O_3	K_2O	Na_2O	SO_3	MgO	TiO_2	Mn_3O_4
PC	64.60	20.08	4.98	3.24	0.53	0.27	3.13	1.98	0.30	0.10
LP	89.56	4.36	1.00	1.60	0.34	0.21	–	1.01	0.06	1.61
nS	0.08	98.68	0.37	–	0.35	0.32	–	–	0.01	–

Table 2
Product information and molecular weight of superplasticizers.

No.	Dry matter	Colour	Density (g/cm^3)	pH	Chloride content	Alkali content	Mass average molecular weight M_w (g/mol)	Number-average molecular weight M_n (g/mol)	PDI (M_w/M_n)
SP1	35%	Amber	1.11	5.9	≤0.1%	≤3%	49500	21806	2.27
SP2	25%	Light brown	1.05	5.2	≤0.1%	≤1.5%	87600	39459	2.22
SP3	35%	Yellowish	1.07	4.2	≤0.1%	≤0.5%	59700	26300	2.27
SP4	40%	Yellowish	1.09	4.1	≤0.1%	≤1%	40700	20765	1.96

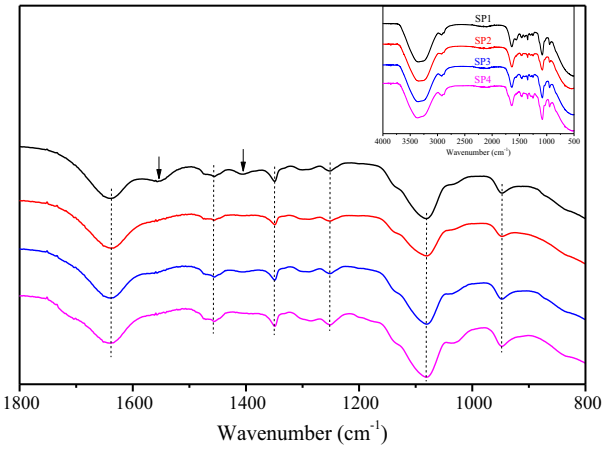

Fig. 2. FTIR spectra of PCEs.

SP1 and SP3 at different concentrations. All samples were mixed manually and vibrated for about 8 min before test. Furthermore, the correlation between zeta potential and pH is determined.

2.3.2. Flowability and slump flow life

The spread flow of pastes and UHPCs were measured by using a truncated conical mould (Hägermann cone: height 60 mm, top diameter 70 mm, bottom diameter 100 mm) without jolting, in accordance with EN 1015–3: 2007. The pastes were utilized with four different SPs at the dosage varying from 0.4% to 2.0%, while the UHPCs incorporated the SPs with the dosage from 1.0% to 3.0%. It should be pointed out that the samples were mixed with tap water at w/p ratio of 0.2, and the water temperature has slight variation at different seasons. So, this may have an influence on the spread flow [36].

To evaluate the fluid-retaining ability and slump flow life of UHPC, the spread flow of UHPCs were measured till 4 h after the sample preparation. The samples were stored at room temperature of about 20 ± 1 °C and a plastic film was used to cover the mixing bowl to prevent moisture loss after each measurement. The measurement was performed with a regular time interval, and the UHPC was mixed for about 20 s before each measurement. To analyse the SP dosage effect, UHPC samples were tested at SP dosages of 2.2% and 2.6% respectively, with a w/p ratio of 0.2. Then, to evaluate the water content sensitivity, the w/p ratios were increased to 0.22 at the SP dosage of 2.2%.

2.3.3. Reaction kinetics

To analyse the effect of superplasticizer on the hydration kinetics, an isothermal calorimeter (TAM Air, Thermometric) is employed to measure the heat evolution of UHPC pastes, with the set temperature of 20 °C. The samples were mixed manually, and then vibrated to ensure a good homogeneity. The prepared pastes were filled into an ampoule which is then loaded to the calorimeter, which means that the sampling time (4–6 min) was not recorded. The samples were fixed at w/p ratios of 0.2, and added four different types of SP at the dosage of 0.4%, 0.8%, 1.2%, 1.6% and 2.0%, respectively.

2.3.4. Setting time

The setting times of pastes were evaluated by using the Vicat apparatus based on EN 196–3: 2005. The w/p ratios for all pastes were fixed at 0.2. The PCE-type SPs were added to the pastes at the dosage of 0.4%, 0.8% and 1.2%, respectively. The setting time was tested under the room temperature of approximately 20 ± 1 °C.

2.3.5. Chemical and autogenous shrinkage

The chemical shrinkage of pastes was tested by a vial-capillary setup based on ASTM C 1608–05, completely filled by paraffin oil without water in the capillary tube in order to keep the w/p ratio at constant of 0.2. The autogenous shrinkage of pastes was obtained by using the digital dilatometer bench and sealing corrugated tubes following ASTM C 1698–09, while the zero-time of measurement was defined as the final setting time. The samples were firstly tested under different SP types with a constant dosage of 0.8%, then the samples containing SP3 with different dosages (0.4% and 1.2%) were measured. All the specimens were stored at room temperature (20 ± 1 °C) and data were collected for 72 h.

2.3.6. Strength

The fresh UHPC, with the w/p ratio of 0.2, was cast into plastic moulds ($40 \times 40 \times 160\ mm^3$), and covered with plastic film to prevent moisture loss. All the samples were demoulded approximately 24 h after casting and then cured in water under room temperature of 20 ± 1 °C. The compressive and flexural strength of UHPC samples were tested after 1 day, 3 days, and 7 days respectively, based on EN 196–1: 2005. To investigate the SP type effect on the early age strength, the UHPCs were cast with all SPs under dosage of 2.2% (close to saturation dosages). Then, the UHPCs were also prepared using SP3 with a dosage of 1.8%, 2.6% and 3.0%, respectively.

3. Results

3.1. Zeta potential

The zeta potential measurement has been proven to be an effective method to characterise the interaction between powder particles and PCEs [13,37–40]. Fig. 3 shows the pH and zeta potential of

Table 3
Mass proportion of paste and UHPC reference mixtures.

Mixtures	Materials					
	PC	LP	MS	S	nS	w/p
Paste	1.000	0.4464	0	0	0.0417	0.2
UHPC	1.000	0.4464	0.3720	1.7857	0.0417	0.2–0.22

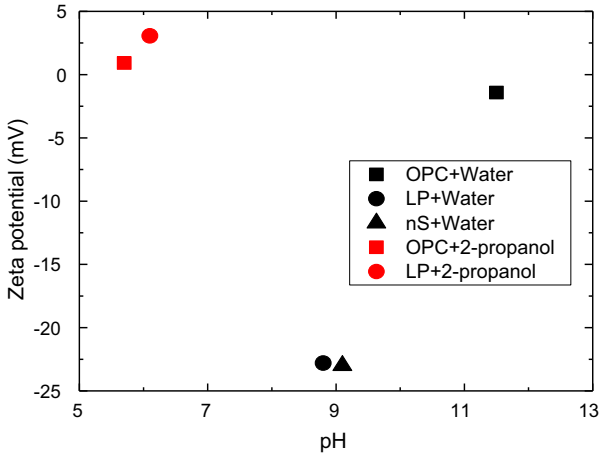

Fig. 3. Zeta potential of particles without SP.

the particles in water and organic solvent (2-propanol). The cement suspension in water shows a high pH, and is slightly acidic in 2-propanol. The zeta potential changes from −1.42 mV to 0.91 mV. The limestone powder and nano-silica have a similar pH and zeta potential in water, approximately 9 and −23 mV, respectively. The limestone powder in 2-propanol shows a comparable result to cement, about 6.1 (pH) and 3.1 mV (zeta potential). The pure cement particles in water without PCE shows a negative zeta potential, which is in line with the reported researches [37,38,40,41]. Nevertheless, some researchers reported a positive zeta potential for cement pastes without SP, and then it changes from positive to negative with the addition of SP [12,15,39]. These differences may be caused by the particle concentration, chemical composition, conductivity, ion characteristic and pH value of suspension, and testing methods. Normally, higher magnitudes of zeta potential values occur at higher cement concentrations [38,42]. Lower zeta potentials could be caused by high pH and high clinker phases of C_3S and C_2S, while higher contents of Ca^{2+}, C_3A and C_4AF lead to relatively higher zeta potentials [37,43]. The limestone powder and nano-silica have higher negative zeta potentials than cement in water, which may indicate that they generate more anions in water. As a similar explanation, it was also pointed out that a great amount of silica powder could produce a large amount of dissociated silanol site [SiO^-], which results in higher negative zeta potentials [37].

Fig. 4 presents the zeta potential of different powder suspensions with SP1 and SP3. With the addition of SP, the zeta potential of cement suspension decreases sharply, due to the adsorption of carboxylic acids groups on cement particles. Conversely, the zeta potential values of limestone powder and nano-silica suspension have a rapid increase. These increases are probably caused by the better adsorption ability and lower charge density of PCE molecules than the previous anions on the particles. A similar hypothesis was used to explain the relationship between zeta potential of synthesized ettringite and PCE concentration [44]. With the continuous increase of SP, all suspensions tend to be stable beyond SP concentrations of 0.05 g/L, which confirms the existence of saturation dosages. Because no further PCE molecules are adsorbed on particles above the saturation dosage, which contributes to unchanged zeta potential.

3.2. Spread flow and water demand of paste

The critical dosage of SP can be defined as the dosage that begins to provide obvious dispersing effect, while the saturation dosage means that the fluidity will not or just change very slightly beyond this dosage [11]. Fig. 5(a) depicts the spread flow of pastes incorporating different types and dosages of SP. The relationship between the flow ability of pastes and SP dosages shows an exponential trend in this study, which means the spread flow diameters have a rapid increase at relatively low dosages of SP, and then typical plateaus occur after the saturation dosages. It shows that the maximum flow diameters of pastes with different SP types are approximately 35 cm. The critical (saturation) dosages of SP1, SP2, SP3 and SP4 for paste are approximately 0.6% (1.4%), 0.4% (0.8%), 0.6% (1.2%) and 0.4% (1.2%), respectively. It can be concluded that SP2 and SP3 have a much higher dispersing ability for pastes with dosages ranging from 0.4% to 1.2%. However, with the increase of SP dosages, the dispersing ability of SP3 and SP4 are only a bit higher than that of SP2 and SP1.

To reduce the porosity, it is necessary to limit the w/p for a fluid paste at a certain dosage of SP. To investigate the effect of SP on the water demand of UHPC paste, the relative slump Γ_p was calculated according to Okamura and Ozawa [45,46]:

$$\Gamma_p = \left(\frac{d}{d_0}\right)^2 - 1;\ d = \frac{d_1 + d_2}{2} \tag{1}$$

where d_1 and d_2 are the perpendicular diameters of the spread flow, d_0 is the cone base diameter (100 mm). The relative slump can be plotted versus w/p and a linear trend line can be plotted thus [47,48]:

$$\frac{V_w}{V_p} = \beta_p + E_p\Gamma_p \tag{2}$$

where V_w and V_p represents the volume of water and powder. β_p is as water demand and represents the minimum water content to assure a fluid paste. The deformation coefficient (E_p) is derived from

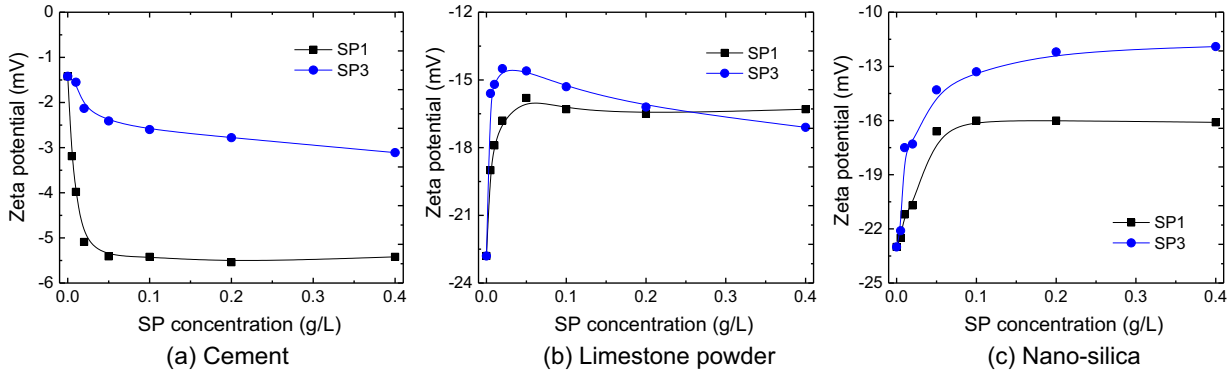

Fig. 4. Zeta potential of particles with SPs.

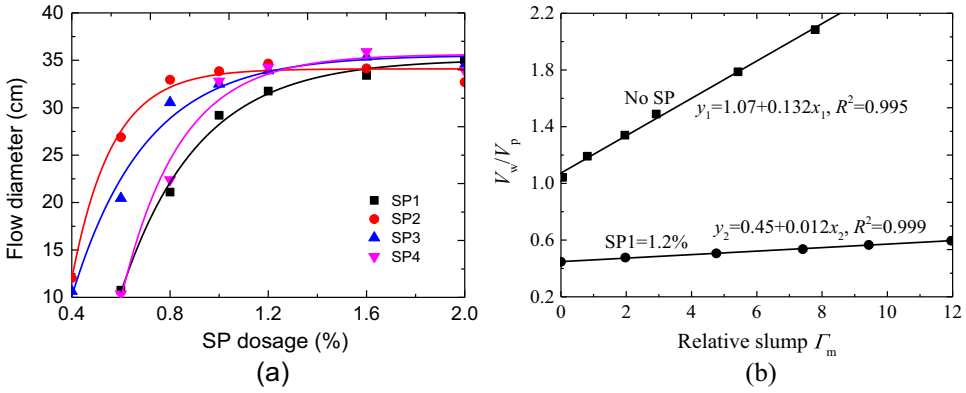

Fig. 5. Spread flow and water demand of pastes.

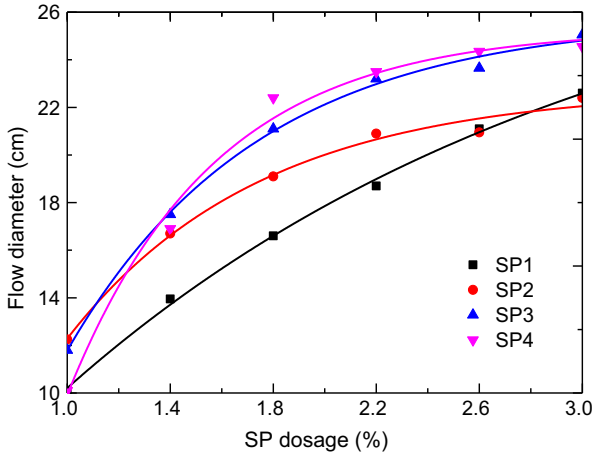

Fig. 6. Spread flow of UHPCs versus SP dosage.

the slope of the linear regression line, which indicates the sensitivity of the materials on the water demand for a specified workability. In this research, Fig. 5(b) shows that water demand of UHPC paste reduces from 1.07 (without SP) to 0.45 (with enough SP), which means the water reduction of demand water is approximately 58%. It also shows a very small deformation coefficient when using sufficient dosage of SP, which indicates that the relative slump is very sensitive to w/p and will increase dramatically with a further addition of water. Thus, all four PCE-type SPs have a good water reduction ability and it is possible to utilize it to achieve a very low w/p ratio for UHPC.

3.3. Spread flow of UHPC

Fig. 6 presents the spread flows of UHPC incorporating different types and dosages of SP. The spread flows of UHPC with SP2, SP3 and SP4 show a typical plateau at high dosages, which are similar to that of pastes. However, the SP1 presents more like a linear increase, which indicates that SP1 increases the flow ability very slowly at the investigated dosage range. The critical dosages of SP2, SP3 and SP4 for UHPC are similar, about 1.0%, meanwhile the saturation dosages are about 2.2%. The critical dosage of SP1 for UHPC is approximately 1.0%, but it does not show a clear saturation dosage till 3.0%. Generally, SP3 and SP4 have a higher dispersing ability than SP1 and SP2 for UHPC.

It shows a lower flow diameter of UHPCs than that of pastes at the same dosage of SP, the reduction is particularly high for SP1 and SP2 at the saturation dosage. SP3 shows excellent effect on spread flow in both pastes and concrete. On the contrary, the SP2 presents a good ability on spread flow in pastes, but cannot keep this ability in UHPCs when aggregates are used as well.

3.4. Slump life of UHPC

Fresh concrete is well known to lose its workability with time, which is called "slump flow loss" [14,49,50]. Fig. 7(a) presents the slump life of the fresh UHPC in 4 h. It shows that the UHPCs with SP1 and SP2 have a short slump life, which have a linear decrease relationship between the flow and elapsed time. The UHPC with SP4 can only keep a good slump life for about 1 h, then the spread flow decreases quickly. UHPC with SP3 presents the best slump life, nearly without any slump flow loss in the testing period of 4 h.

Fig. 7(b) shows the spread flow of the UHPCs within 4 h above the saturation dosages. Compared to the results shown in Fig. 7 (a), the fluid-retaining abilities are not improved or just have a slight increase for SP4 after 2 h, which indicates that the further addition of PCEs cannot increase the slump life. Beyond the saturation dosages of SPs, the completed surface coverage of particles has already been produced and it will not adsorb the PCEs anymore, which results in the same fluid-retaining ability. It also indicates that the slump life is mainly dependent on the adsorbed PCEs rather than PCEs in aqueous solution. Nevertheless, the retention effects can be enhanced greatly when a slightly more amount of water is added, as shown in Fig. 7(c), indicating a very sensitive role of water in UHPC. More alite hydrates and more Ca^{2+} ions are generated, and lime saturation in the pore solution increases, which will retard the hydration and then enhance the fluidity retention [14].

3.5. Hydration kinetics of paste

To understand the retardation effect of superplasticizers, time-dependent normalized heat flow from UHPC pastes with different types and dosages of SPs were recorded by isothermal calorimetry tests, as shown in Fig. 8. Compared to the other three SPs, the SP1 exhibits the largest retardation effect, and the SP2 shows the smallest delay, while the SP3 and SP4 possess a medium retardation effect. It indicates that the four PCEs have different adsorption abilities due to the different chemical structures, and subsequently show different retardation effects on hydration. It is demonstrated from Fig. 8(e) that a higher dosage of PCE always delays the hydration more, and the delay effect continuously increases even after the PCE addition exceeding the saturation dosages (shown in Fig. 5(a)). It indicates that not only the adsorbed PCE but also the

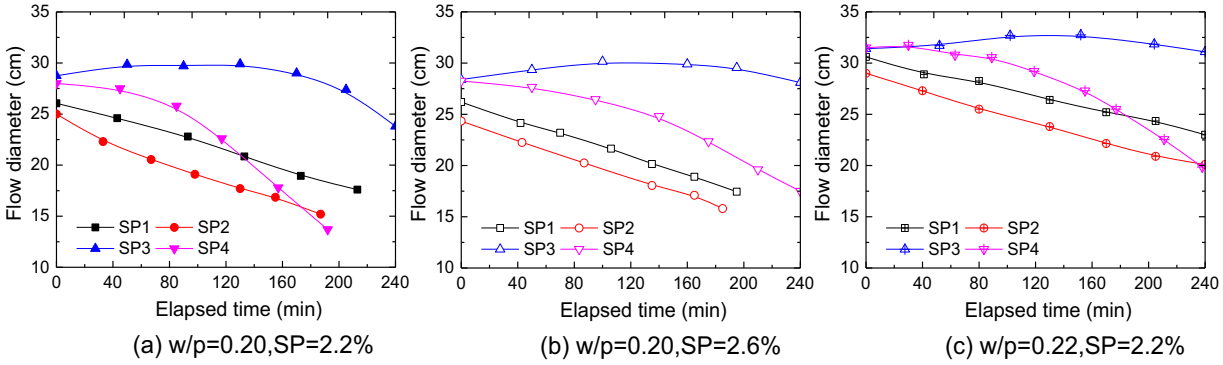

Fig. 7. Spread flow of UHPCs versus time.

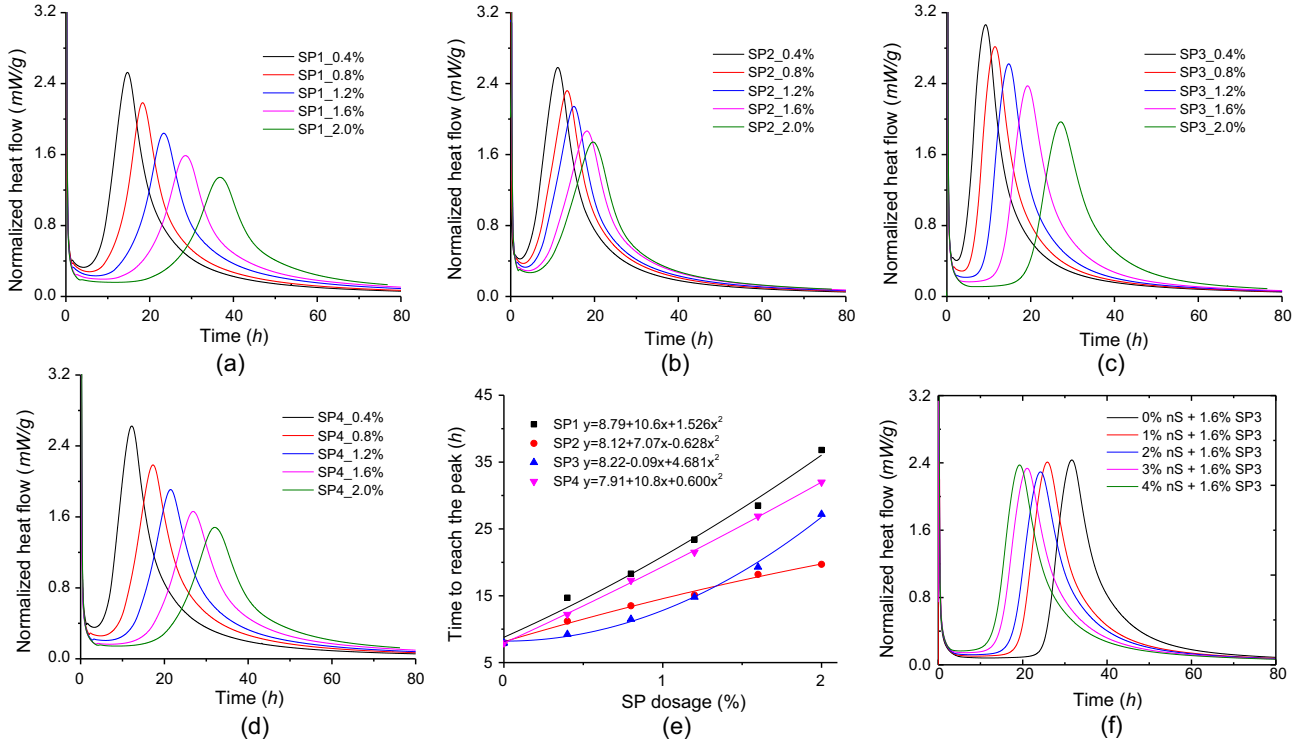

Fig. 8. Calorimetry test results of pastes.

PCE remaining in the aqueous phase contributes to retarding cement hydration [15,17].

Fig. 8(f) gives the normalized heat flow of pastes using different contents of nano-silica. The normalized heat flow curves indicate the time to reach the peak (TTRP) reduces from about 40 h to 20 h, with the increase of nano-silica addition from 0 to 4%. Nano-silica can act as nucleation sites for the precipitation of hydration products, thus accelerating the hydration reactions of cement [47]. Thus, it is feasible to add an appropriate content of nano-materials to decrease the retardation effect when a high dosage of PCE is used. In this study, 3% of nano-silica is observed to be the optimal content on providing an accelerating effect on the hydration process.

3.6. Setting time of paste

Fig. 9 presents the initial and final setting times of pastes incorporating SP1, SP2, SP3 and SP4. It is obvious that the setting times are affected by both SP types and dosages. For all those four SPs, high dosages always increase the setting times. It is also clear that pastes with SP1 have the longest setting times, reaching at about 7.8 h of initial and 11.2 h of final setting time at a dosage of 1.2%. The pastes with SP2 show the shortest setting times, which are approximately 4.25 h (6.5 h) of initial (final) setting time at the dosage of 1.2%. Compared with SP1 and SP2, medium setting times are observed for the pastes containing SP3 and SP4.

3.7. Early-age shrinkage of paste

The early-age shrinkages of UHPC, including the chemical and autogenous shrinkage, are particularly high because of the low w/p and large amount of powders [51,52]. Those shrinkages producing early-age cracks have been important issues for structural concretes, especially for their long-term durability, which are mainly resulted from moisture loss and self-desiccation [20,53]. Usually, the chemical and autogenous shrinkage of cement is considered as an internal (absolute) and external (apparent) volume reduction, respectively. Some researchers believe that the initial

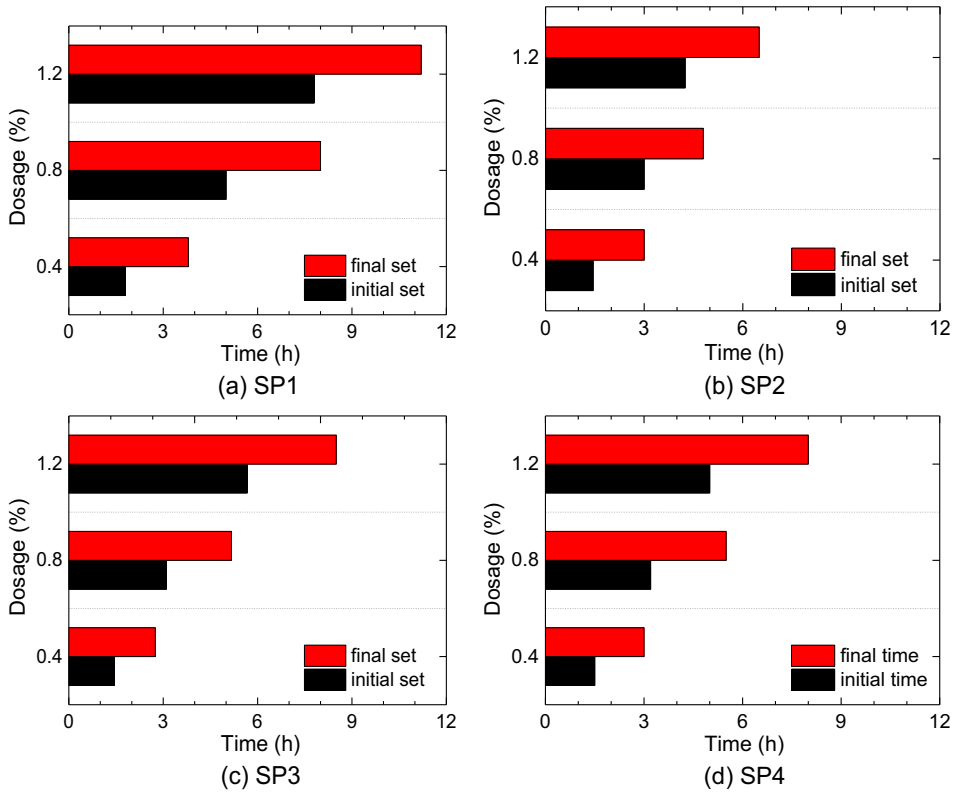

Fig. 9. Setting time of pastes.

cracking may already exist due to autogenous shrinkage [52]. If it is free, the autogenous shrinkage deformation increases as hydration progresses after the final setting. If it is restrained, significant tensile stress and cracks may arise.

Fig. 10(a) shows the chemical shrinkages of pastes with different SP types, while Fig. 10(b) presents the chemical shrinkages of pastes incorporating different dosages of SP3. It is obvious that different types of PCE mainly influence the chemical shrinkage development rate before 24 h, after that they are almost the same. Incorporating a higher dosage of PCE, the paste shows a slower development rate of chemical shrinkage before 24 h.

Fig. 11(a) and (b) present the autogenous shrinkage of pastes with different SP types and dosages, respectively. It can be concluded that SP3 and SP4 contribute to a smaller absolute value of autogenous shrinkage than that of SP1 and SP2. The absolute value of autogenous shrinkage decreases continuously from 0.4% to 1.2% of SP3.

3.8. Early-age strength of UHPC

The retardation effect of PCE polymers leads to the delay of the hydration process, which would consequently lead to a slower development of early-age strength of UHPC. Fig. 12(a) presents the compressive strengths of UHPC with different SPs at a fixed dosage of 2.2%. The 1-day compressive strengths of the UHPCs containing different types of SPs are about 3.2 MPa, 71.1 MPa, 70.9 MPa, and 46.6 MPa, respectively. The 3-day and 7-day compressive strengths are approximately close to 80.9 MPa and 93.3 MPa, respectively. Fig. 12(b) shows the compressive strength of UHPC with SP3 at different dosages. With the increase of SP3

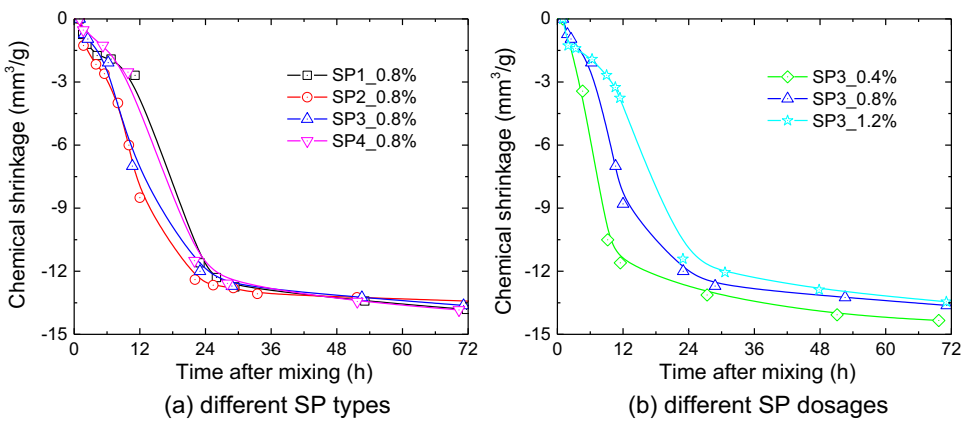

Fig. 10. Chemical shrinkage of pastes.

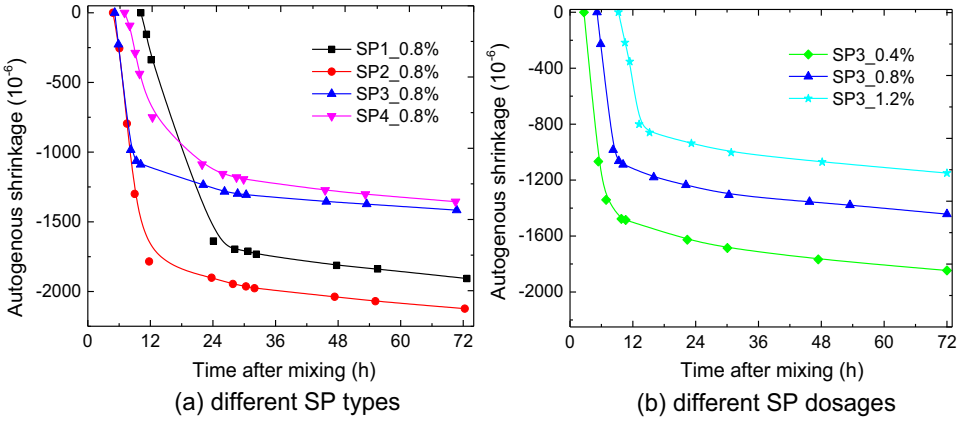

Fig. 11. Autogenous shrinkage of pastes.

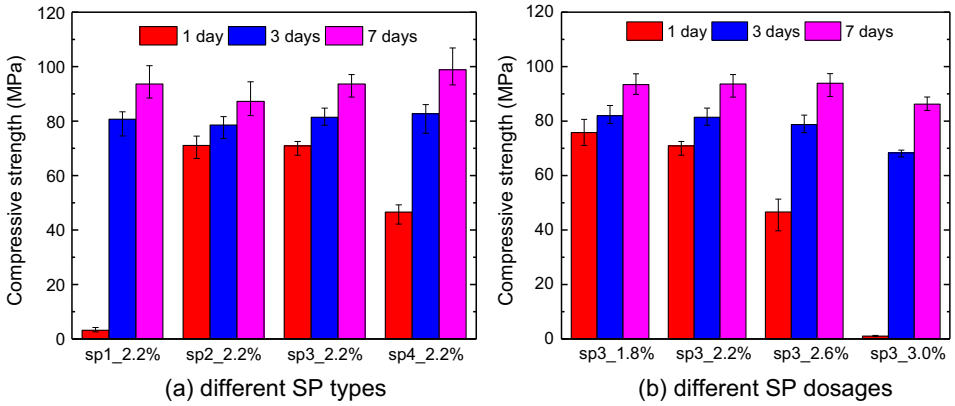

Fig. 12. Compressive strength of UHPCs.

dosage, the 1-day compressive strengths sharply decrease from 75.8 MPa to 1.1 MPa. While the 3-day compressive strengths have a smaller difference, changing from 82.0 MPa to 68.3 MPa. The 7-day compressive strengths are all near to 91.8 MPa. It can be concluded that different types and dosages of SPs contribute to a large different early-age strength development, especially for 1-day strength. The differences become smaller after 3 days, and comparative strengths are obtained after 7 days.

4. Discussion

4.1. Dispersing and fluid-retaining ability

It is believed that the dispersing forces between particles are generated by steric hindrance and electrostatic force after adsorption of PCE-type SP molecules [12,15]. Some researchers noted that the PCE-type SP begins to disperse the particles when it causes the zeta-potential of the pastes to change [40]. A larger magnitude negative value of zeta potential means a higher electrostatic repulsion, which may contribute to a higher fluidity [39]. Obviously, the suspensions of all powders with SP1 have more negative zeta potentials than that of SP3 (see Fig. 4), which means that SP1 has a larger electrostatic repulsion force than SP3. However, SP1 has a worse dispersing ability than SP3, as seen in Fig. 5 and Fig. 6. Thus, the dispersing ability of PCE-type SP is more dependent on the steric hindrance of adsorbed molecules rather than the electrostatic repulsion force.

The amount of adsorbed molecules depends on their structure and dosages, and a higher adsorption on particle surface usually occurs with a higher molecular weight, lower side chain density and shorter side chains [13,18]. The typical plateau occurs after the saturation dosage as shown in Fig. 5, whose existence is confirmed by the results of zeta potential of particles (see Fig. 4). This typical plateau at high dosages can be also observed from the relationships between the SP adsorption on particles and SP dosages [11,15,18,54]. It manifests that SP works only after the adsorption on the particles, which corresponds to the surface coverage [11,55]. When the used SP reaches the saturation dosage, a complete surface coverage will be obtained. Then the dispersing ability of SP will not increase anymore, which results in the occurrence of the typical plateau at high dosages.

Fig. 6 shows considerably lower flow diameters at the same dosage usage of all SPs compared to the results shown in Fig. 5 (a), owing to the addition of aggregates. The decrease tendency of flow is possibly due to the high content of clay inside the used micro-sand by X-ray diffraction analysis, which can occur as an impurity in aggregates [56]. The clay can absorb SP and free water, and then the spread flow is reduced. The negative influence of clay on flow ability might originate from the following aspects: 1) the clay can absorb the free water and reduce the spread flow; 2) some clays (e.g. kaolinite clay) reduce the dispersing effectiveness of SP due to strong electrostatic interaction or formation of clay-PCE "network" via hydrogen bonding [25]; 3) some clays (e.g. montmorillonite clay) exhibit much higher affinity for PCE than cement, which means the adsorption of SP on powders will be decreased [27,28]. Some researchers suggested modifying the polyethylene oxide side chain to obtain a more clay tolerant PCE [26]. It is worth to point out that SP2 possesses the best dispersing ability for paste

below the saturation dosage, but has a relatively weak dispersing ability for UHPC. It indicates that SP2 has a poor adsorption effect on UHPC than on paste, which indicates that SP2 is incompatible with the micro-sand in this study.

The fluid-retaining ability is an important index to describe the workability of concrete, which is usually measured by slump flow loss. The previous researches imply that slump flow loss involves chemical and physical processes [14], which is mainly attributed to the w/p ratio, type and dosage of SP, as well as SO_3 content, alkali content, C—S—H formation, charge characteristic, C_3S/C_2S ratio [14,57,58]. UHPC with SP1 has the shortest slump life, even though SP1 shows the highest retardation effect on the paste setting. The possible reason is that SP1 has a low adsorption ability, which induces an uncompleted surface coverage. Uncompleted surface coverage (below saturation dosage) results in a rapid stiffening of the concrete [11]. UHPC with SP2 has a poor slump life probably due to its weak retardation effect on paste hydration and uncompleted surface coverage. The UHPC with SP3 shows an excellent slump life in the whole testing time (4 h) because of good adsorption ability. UHPC with SP4 can maintain a good slump life up to 1 h, which then experiences a sharp decrease after that time. The fluid-retaining ability is mainly determined by the adsorbed PCEs rather than the PCEs in the aqueous solution, which is similar to the dispersing ability.

4.2. Retardation effect

The retardation effect of SP can be observed and reflected by the hydration kinetics and setting of pastes, as well as flow retention and early-age strength development of concretes. Some researchers described the retardation effect of PCEs as following: adding PCEs prevents solid phase nucleation and hydration products growths, then leads to retardation of cement hydration [13].

The results of hydration kinetics of pastes show that the retardation effects of PCEs on hydration are greatly attributed by types and dosages of PCEs. It should be noted that the normalized heat flow of all pastes (approximately 1.2%) is still delayed after saturation dosage (Fig. 8). It indicates the retardation effect is not only affected by the adsorbed PCEs but also the PCEs in the aqueous phase, which is different from the mechanism of fluid-retaining effect. Generally, a larger retardation effect is probably resulted from a shorter side chain [26], higher concentrations of the carboxylic groups in the aqueous phase, higher adsorption amount of PCE on cement particle, and different charge characteristics of SP molecules ($-COO^- > -SO_3^- > \equiv N^+ -$) [29]. Some researchers illustrated the retarding effect of PCEs to three aspects [15,59]: 1) hindering the diffusion of water and ions at the particle-solution interface by adsorbed polymer layers; 2) inhibiting the nucleation and precipitation of hydrates through chelating the Ca^{2+} ions in the aqueous solution by $-COO^-$ groups in PCE molecules; 3) changing the growth kinetics and morphology of hydrate phases by better dispersion of particle grains.

From the results of setting time of pastes, it indicates that those PCEs have a retardation effect on the setting of pastes, and the retardation effect is higher with the increase of SP dosages. The results indicate that SP1 is not suitable to obtain a high early age strength for paste or concrete due to the high retardation effect, which is confirmed by the strength results as shown in Fig. 12. The low retardation effect of SP2 makes it possible to achieve a relatively high early age strength for paste or concrete.

From the early-age strength development point of view, it is obvious to observe the retardation effect of PCEs on the development of strength during the early curing age. The retardation effect on the early-age strength of UHPC is in line with the results form hydration kinetics and setting times of paste. A higher dosage always shows a lower strength before 3 days, and the differences turn to be smaller with the increasing curing time. From Fig. 12, it also indicates that the retardation effect has limited influence on the strength development after 3 days.

4.3. Physical and chemical process effects

4.3.1. Correlation between final setting and hydration

Some researchers pointed out that the final setting time of paste (t_{final}) is closest to the inflection point of the heat flow curve in the accelerating stage, which means the correlation coefficient is close to 1.0 [60]. To analyse the correlation and understand the physical meaning of the inflection point, the first derivative of the heat flow curve $\ddot{Q}(t)$ is calculated by:

$$\ddot{Q}(t) = \frac{\partial \dot{Q}(t)}{\partial t} \tag{3}$$

where $\ddot{Q}(t)$ is the heat flow rate [J/s^2], $\dot{Q}(t)$ is the heat flow [J/s], t is the time [s]. As shown in Fig. 13, these heat flow rate curves can be interpreted as the energy acceleration curves, which was also observed by Schmidt [60]. The vertical lines present the times $t_{\ddot{Q}=max}$ under the maximum heat flow rates (inflection points of the accelerated heat flow curves).

The relationship between t_{final} and $t_{\ddot{Q}=max}$ of all pastes are shown in Fig. 13(c). Linear relationships for all PCEs under different dosages are observed, which means that there is a good correlation between t_{final} and $t_{\ddot{Q}=max}$. Meanwhile, the four linear trend lines cross the same point at (4.6, 0.9), which represents the theoretical value of t_{final} versus $t_{\ddot{Q}=max}$ of paste without SP. A time difference between t_{final} and $t_{\ddot{Q}=max}$ clearly exists, which changes with different type and dosage of PCE. These differences occur due to different mechanisms for setting and hydration kinetics of pastes. Namely, hydration is mainly affected by chemical processes, while the setting time is determined by both a chemical process and physical coagulation, especially under the use of PCEs. The physical coagulation effect makes the t_{final} smaller than $t_{\ddot{Q}=max}$, and a larger time difference indicates a higher physical coagulation effect. A smaller slope of the trend line indicates that the SP has a larger delay effect on the chemical process than the physical coagulation.

4.3.2. Correlation between shrinkage and retardation

The chemical shrinkage of paste is generated by the absolute volume change during the hydration. Therefore, it should be influenced by the retardation effect of PCEs on the hydration of paste, which is mainly determined by chemical process. Comparing the results shown in Fig. 8 and Fig. 10, there is a correlation between chemical shrinkage and hydration delay, a longer delay results in a faster developing rate of chemical shrinkage before about 24 h. After that, the chemical shrinkages are almost the same, which indicates that the retardation of PCEs mainly affects the hydration rate in the early age, and possesses little influence on the final total hydration, which is consistent with the findings of the early-age strength development of UHPC.

The autogenous shrinkage of pastes was measured based on the final setting time, which was considered as the zero time of autogenous shrinkage. Hence, the autogenous shrinkage results are affected by the retardation effect of PCEs on the setting of paste, namely, both chemical process and physical coagulation. For the pastes with the same type of PCEs, the absolute autogenous shrinkage value can be reduced with the increase of SP dosage, as seen from Fig. 11(b), which means a slower physical coagulation and chemical process within a certain period could result in a smaller autogenous shrinkage. However, there is no obvious correlation between autogenous shrinkage and setting with the addition of

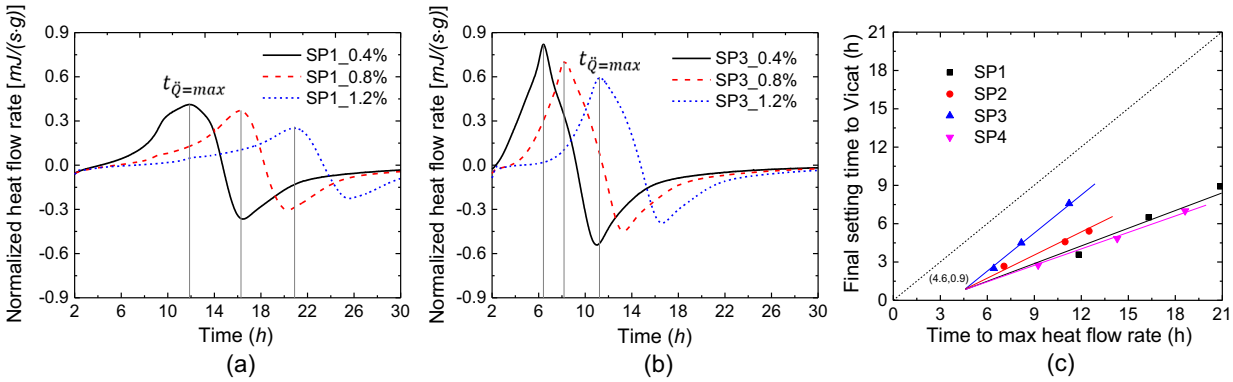

Fig. 13. Normalized heat flow rates and t_{final} versus $t_{\dot{Q}=max}$.

different type of PCEs from Fig. 11(a). This is probably because the physical coagulation and chemical process have different influences on the final setting time and autogenous shrinkage.

5. Conclusions

This paper investigates the effect of PCE-type SP on the early-age behaviour of UHPC. Zeta potential of powder suspensions, setting, hydration kinetics, early-age shrinkages, spread flow and water demand of pastes, spread flow, slump life and early-age strength development of UHPC were measured. The dispersing and fluid-retaining ability, retardation effect of PCEs, as well as physical coagulation and chemical processes with PCEs were analysed and discussed. The results indicate that appropriate types and dosages of PCE-type SP should be carefully selected for the design of UHPC. Based on the obtained results, the following conclusions can be drawn:

- The zeta potential of different powder suspension shows large differences under the addition of PCE-type SP. It confirms the existence of the saturation dosages and shows steric hindrance as the main influence factor on the dispersing ability of PCE-type SP.
- The dispersing ability of PCE-type SP is greatly dependent on its chemical structure and adsorption ability on particles. The flowability of paste increases continuously from critical dosage to saturation dosage and remains constant after obtaining a complete surface coverage of particles above the saturation dosage.
- The fluid-retaining ability is mainly determined by the adsorbed PCEs and it will not increase after saturation dosages of SPs due to the complete coverage of particles, but the water content plays a very sensitive role on the fluid-retaining ability of UHPC.
- Both the adsorbed PCEs and the PCEs remaining in the aqueous phase contribute to the retardation effect. The retardation effect mainly influences the early-age strength before 3 days. 3% of nano-silica as cement replacement is found as the optimal content to reduce the retardation effect.
- A linear correlation between t_{final} and $t_{\dot{Q}=max}$ is observed. The $t_{\dot{Q}=max}$ is mainly resulting from chemical process, while the t_{final} can be influenced by both chemical process and physical coagulation.
- The chemical shrinkage of paste is mainly generated by chemical processes, which only influence the chemical shrinkage developing rate for about 1 day with PCEs. But autogenous shrinkage is affected by both physical coagulation and chemical processes.

Acknowledgements

This research was carried out under the funding by China Scholarship Council and Eindhoven University of Technology. Furthermore, the authors wish to express their gratitude to the following sponsors of the Building Materials research group at TU Eindhoven: Rijkswaterstaat Grote Projecten en Onderhoud; Graniet-Import Benelux; Kijlstra Betonmortel; Struyk Verwo; Attero; Enci; Rijkswaterstaat Zee en Delta-District Noord; Van Gansewinkel Minerals; BTE; V.d. Bosch Beton; Selor; GMB; Icopal; BN International; Eltomation, Knauf Gips; Hess AAC Systems; Kronos; Joma; CRH Europe Sustainable Concrete Centre; Cement & Beton Centrum; Heros; Inashco; Keim; Sirius International; Boskalis; NNERGY; Millvision; Sappi and Studio Roex (in chronological order of joining).

References

[1] P. Richard, M. Cheyrezy, Composition of reactive powder concretes, Cem. Concr. Res. 25 (1995) 1501–1511.
[2] P. Prem, B. Bharatkumar, N. Iyer, Mechanical properties of ultra high performance concrete, Int. J. Civil, Environ. Struct. Constr. Archit. Eng. 6 (2012) 1680–1689.
[3] D.Y. Yoo, N. Banthia, Mechanical properties of ultra-high-performance fiber-reinforced concrete: a review, Cem. Concr. Compos. 73 (2016) 267–280.
[4] S. Abbas, A.M. Soliman, M.L. Nehdi, Exploring mechanical and durability properties of ultra-high performance concrete incorporating various steel fiber lengths and dosages, Constr. Build. Mater. 75 (2015) 429–441.
[5] W. Wang, J. Liu, F. Agostini, C.A. Davy, F. Skoczylas, D. Corvez, Durability of an ultra high performance fiber reinforced concrete (UHPFRC) under progressive aging, Cem. Concr. Res. 55 (2014) 1–13.
[6] H. Wu, Q. Fang, J. Gong, J.Z. Liu, J.H. Zhang, Z.M. Gong, Projectile impact resistance of corundum aggregated UHP-SFRC, Int. J. Impact Eng. 84 (2015) 38–53.
[7] R. Yu, L. van Beers, P. Spiesz, H.J.H. Brouwers, Impact resistance of a sustainable ultra-high performance fibre reinforced concrete (UHPFRC) under pendulum impact loadings, Constr. Build. Mater. 107 (2016) 203–215.
[8] R. Yu, P. Spiesz, H.J.H. Brouwers, Development of ultra-high performance fibre reinforced concrete (UHPFRC): towards an efficient utilization of binders and fibres, Constr. Build. Mater. 79 (2015) 273–282.
[9] C. Shi, Z. Wu, J. Xiao, D. Wang, Z. Huang, Z. Fang, A review on ultra high performance concrete: Part I. Raw materials and mixture design, Constr. Build. Mater. 96 (2015) 368–377.
[10] S.-T. Kang, Y. Lee, Y.-D. Park, J.-K. Kim, Tensile fracture properties of an ultra high performance fiber reinforced concrete (UHPFRC) with steel fiber, Compos. Struct. 92 (2010) 61–71.
[11] R.J. Flatt, I. Schober, Superplasticizers and Rheology of Concrete, Woodhead Publishing Limited, 2011.
[12] C.Z. Li, N.Q. Feng, Y. De Li, R.J. Chen, Effects of polyethlene oxide chains on the performance of polycarboxylate-type water-reducers, Cem. Concr. Res. 35 (2005) 867–873.
[13] Y. Li, C. Yang, Y. Zhang, J. Zheng, H. Guo, M. Lu, Study on dispersion, adsorption and flow retaining behaviors of cement mortars with TPEG-type polyether kind polycarboxylate superplasticizers, Constr. Build. Mater. 64 (2014) 324–332.

[14] S. Chandra, J. Björnström, Influence of superplasticizer type and dosage on the slump loss of Portland cement mortars – Part II, Cem. Concr. Res. 32 (2002) 1613–1619.
[15] Y. Zhang, X. Kong, Correlations of the dispersing capability of NSF and PCE types of superplasticizer and their impacts on cement hydration with the adsorption in fresh cement pastes, Cem. Concr. Res. 69 (2015) 1–9.
[16] P.-C. Nkinamubanzi, S. Mantellato, R.J. Flatt, Superplasticizers in Practice, Elsevier Ltd, 2016.
[17] K. Yamada, T. Takahashi, S. Hanehara, M. Matsuhisa, Effects of the chemical structure on the properties of polycarboxylate-type superplasticizer, Cem. Concr. Res. 30 (2000) 197–207.
[18] F. Winnefeld, S. Becker, J. Pakusch, T. Götz, Effects of the molecular architecture of comb-shaped superplasticizers on their performance in cementitious systems, Cem. Concr. Compos. 29 (2007) 251–262.
[19] W. Schmidt, H.J.H. Brouwers, H.-C. Kuehne, B. Meng, Effects of the characteristics of high range water reducing agents and the water to powder ratio on rheological and setting behavior of self-consolidating concrete, Adv. Civil Eng. Mater. 3 (2015) 1–15.
[20] D.P. Bentz, A review of early-age properties of cement-based materials, Cem. Concr. Res. 38 (2008) 196–204.
[21] B. Felekoğlu, H. Sarikahya, Effect of chemical structure of polycarboxylate-based superplasticizers on workability retention of self-compacting concrete, Constr. Build. Mater. 22 (2008) 1972–1980.
[22] J.Y. Shin, J.S. Hong, J.K. Suh, Y.S. Lee, Effects of polycarboxylate-type superplasticizer on fluidity and hydration behavior of cement paste, Kor. J. Chem. Eng. 25 (2008) 1553–1561.
[23] A. Hallal, E.H. Kadri, K. Ezziane, A. Kadri, H. Khelafi, Combined effect of mineral admixtures with superplasticizers on the fluidity of the blended cement paste, Constr. Build. Mater. 24 (2010) 1418–1423.
[24] C. Schröfl, M. Gruber, J. Plank, Preferential adsorption of polycarboxylate superplasticizers on cement and silica fume in ultra-high performance concrete (UHPC), Cem. Concr. Res. 42 (2012) 1401–1408.
[25] L. Zhang, Q. Lu, Z. Xu, Q. Liu, H. Zeng, Effect of polycarboxylate ether comb-type polymer on viscosity and interfacial properties of kaolinite clay suspensions, J. Colloid Interface Sci. 378 (2012) 222–231.
[26] L. Lei, J. Plank, A concept for a polycarboxylate superplasticizer possessing enhanced clay tolerance, Cem. Concr. Res. 42 (2012) 1299–1306.
[27] S. Ng, J. Plank, Interaction mechanisms between Na montmorillonite clay and MPEG-based polycarboxylate superplasticizers, Cem. Concr. Res. 42 (2012) 847–854.
[28] L. Lei, J. Plank, A study on the impact of different clay minerals on the dispersing force of conventional and modified vinyl ether based polycarboxylate superplasticizers, Cem. Concr. Res. 60 (2014) 1–10.
[29] Y.R. Zhang, X.M. Kong, Z.B. Lu, Z.C. Lu, S.S. Hou, Effects of the charge characteristics of polycarboxylate superplasticizers on the adsorption and the retardation in cement pastes, Cem. Concr. Res. 67 (2015) 184–196.
[30] S.P. Jiang, J.C. Mutin, A. Nonat, Studies on mechanism and physico-chemical parameters at the origin of the cement setting. I. The fundamental processes involved during the cement setting, Cem. Concr. Res. 25 (1995) 779–789.
[31] S.P. Jiang, J.C. Mutin, A. Nonat, Studies on mechanism and physico-chemical parameters at the origin of the cement setting II. Physico-chemical parameters determining the coagulation process, Cem. Concr. Res. 26 (1996) 491–500.
[32] D.P. Bentz, E.J. Garboczi, C.J. Haecker, O.M. Jensen, Effects of cement particle size distribution on performance properties of Portland cement-based materials, Cem. Concr. Res. 29 (1999) 1663–1671.
[33] D.P. Bentz, Cement hydration: building bridges and dams at the microstructure level, Mater. Struct. 40 (2007) 397–404.
[34] D.-Y. Yoo, J.-J. Park, S.-W. Kim, Y.-S. Yoon, Early age setting, shrinkage and tensile characteristics of ultra high performance fiber reinforced concrete, Constr. Build. Mater. 41 (2013) 427–438.
[35] J. Brooks, Shrinkage of Concrete, Butterworth-Heinemann, 2015.
[36] W. Schmidt, H.J.H. Brouwers, H.C. Kühne, B. Meng, Influences of superplasticizer modification and mixture composition on the performance of self-compacting concrete at varied ambient temperatures, Cem. Concr. Compos. 49 (2014) 111–126.
[37] Y. Elakneswaran, T. Nawa, K. Kurumisawa, Zeta potential study of paste blends with slag, Cem. Concr. Compos. 31 (2009) 72–76.
[38] S. Srinivasan, S.A. Barbhuiya, D. Charan, S.P. Pandey, Characterising cement-superplasticiser interaction using zeta potential measurements, Constr. Build. Mater. 24 (2010) 2517–2521.
[39] Y. He, X. Zhang, R.D. Hooton, Effects of organosilane-modified polycarboxylate superplasticizer on the fluidity and hydration properties of cement paste, Constr. Build. Mater. 132 (2017) 112–123.
[40] C.M. Neubauer, M. Yang, H.M. Jennings, Interparticle potential and sedimentation behavior of cement suspensions: effects of admixtures, Adv. Cem. Based Mater. 8 (1998) 17–27.
[41] T. Zhang, S. Shang, F. Yin, A. Aishah, A. Salmiah, T.L. Ooi, Adsorptive behavior of surfactants on surface of Portland cement, Cem. Concr. Res. 31 (2001) 1009–1015.
[42] E. Nägele, U. Schneider, From cement to hardened paste – an elektrokinetic study, Cem. Concr. Res. 19 (1989) 978–986.
[43] K. Yoshioka, E.I. Tazawa, K. Kawai, T. Enohata, Adsorption characteristics of superplasticizers on cement component minerals, Cem. Concr. Res. 32 (2002) 1507–1513.
[44] A. Zingg, F. Winnefeld, L. Holzer, J. Pakusch, S. Becker, L. Gauckler, Adsorption of polyelectrolytes and its influence on the rheology, zeta potential, and microstructure of various cement and hydrate phases, J. Colloid Interface Sci. 323 (2008) 301–312.
[45] M. Hajime Okamura, Ouchi, self-compacting concrete, J. Adv. Concr. Technol. 1 (2003) 5–15.
[46] H.J.H. Brouwers, H.J. Radix, Self-compacting concrete: theoretical and experimental study, Cem. Concr. Res. 35 (2005) 2116–2136.
[47] G. Quercia, G. Hüsken, H.J.H. Brouwers, Water demand of amorphous nano silica and its impact on the workability of cement paste, Cem. Concr. Res. 42 (2012) 344–357.
[48] Q.L. Yu, H.J.H. Brouwers, Microstructure and mechanical properties of β-hemihydrate produced gypsum: an insight from its hydration process, Constr. Build. Mater. 25 (2011) 3149–3157.
[49] A. Mardani-Aghabaglou, M. Tuyan, G. Yilmaz, Ö. Ariöz, K. Ramyar, Effect of different types of superplasticizer on fresh, rheological and strength properties of self-consolidating concrete, Constr. Build. Mater. 47 (2013) 1020–1025.
[50] I. Papayianni, G. Tsohos, N. Oikonomou, P. Mavria, Influence of superplasticizer type and mix design parameters on the performance of them in concrete mixtures, Cem. Concr. Compos. 27 (2005) 217–222.
[51] W. Shen, X. Li, G. Gan, L. Cao, C. Li, J. Bai, Experimental investigation on shrinkage and water desorption of the paste in high performance concrete, Constr. Build. Mater. 114 (2016) 618–624.
[52] H. Mihashi, J.P.D.B. Leite, State-of-the-art report on control of cracking in early age concrete, J. Adv. Concr. Technol. 2 (2004) 141–154.
[53] Y. Li, J. Li, Capillary tension theory for prediction of early autogenous shrinkage of self-consolidating concrete, Constr. Build. Mater. 53 (2014) 511–516.
[54] H. Bessaies-Bey, R. Baumann, M. Schmitz, M. Radler, N. Roussel, Organic admixtures and cement particles: competitive adsorption and its macroscopic rheological consequences, Cem. Concr. Res. 80 (2016) 1–9.
[55] G. Kirby, J.A. Lewis, H. Matsuyama, S. Morissette, J.F. Young, Polyelectrolyte effects on the rheological properties of concentrated cement suspensions, J. Am. Ceram. Soc. 83 (2000) 1905–1913.
[56] A.A. Jeknavorian, L. Jardine, C.C. Ou, H. Koyata, K. Folliard, Interaction of superplasticizers with clay-bearing aggregates, in: Proc. Seventh CANMET/ACI Int. Conf. Superplast. Other Chem. Admixtures Concr. SP-217, 2003, 143–160.
[57] D. Bonen, S.L. Sarkar, The superplasticizer adsorption capacity of cement pastes, pore solution composition, and parameters affecting flow loss, Cem. Concr. Res. 25 (1995) 1423–1434.
[58] Y. Chen, I. Odler, On the origin of Portland cement setting, Cem. Concr. Res. 22 (1992) 1130–1140.
[59] M.Y.A. Mollah, W.J. Adams, R. Schennach, D.L. Cocke, A review of cement-superplasticizer interactions and their models, Adv. Cem. Res 12 (2000) 153–161.
[60] W. Schmidt, Design Concepts for the Robustness Improvement of Self-compacting Concrete: Effect of Admixtures and Mixture Components on the Rheology and Early Hydration at Varying Temperatures, Eindhoven university of technology, 2014.